

Search for Extraplanar Molecular Gas **in NGC 891**

Tiffany Hayes

Thesis Advisor: Dr. Richard Rand
University of New Mexico
2008

Abstract

Disk-halo cycling is an important part of spiral galaxy evolution; in the last few years different phases of gas have been found to exist off of the plane of galaxies. However, there have been conflicting claims about the existence of molecular gas off the plane. Using the Combined Array for Research in Millimeter-wave Astronomy (CARMA) array we observed CO emission from NGC 891. While we did not detect molecular gas off of the plane of NGC 891, we were able to put limits on the size of clouds, if they do exist.

Table of Contents

1. Introduction	4
1.1 The Disk-Halo Connection	4
1.2 NGC 891	5
2. Interferometry	8
2.1 Clean	16
3. Observations	16
4. Reduction	17
5. Results	19
6. Conclusions	23
7. References	30

1. Introduction

Spiral galaxies consist of stars, gas, and dust; the majority of the mass is believed to be in a thin disk a few hundred parsecs thick. The gas can be found in ionized, atomic, molecular and atomic forms, and is mostly hydrogen. Star formation takes place primarily inside giant molecular clouds. However, in the past twenty years of observing, it has been found that about 40% of galaxies have gas extended off of the plane of the galaxy, into the region known as the halo (e.g. Howk & Savage 1999). Most of this gas is in the following forms: diffuse, warm (about $T=10,000$ K) ionized gas, atomic gas (21-cm emission), hot ($T=\text{millions of K}$) ionized gas that emits in the X-ray, and relativistic particles seen through synchrotron radiation. Whether molecular gas has a vertically extended component is the subject of this thesis.

1.1 The Disk-Halo Connection

Norman & Ikeuchi (1989) present a model by which gas in the disk is raised into the halo. It is known that stars form in clusters, and so supernova explosions are also clustered. The multiple supernovae in a cluster sweep up the ambient gas and dust into large "supershells" that are filled with hot, high-pressured gas, pushing the interstellar medium (ISM) out. If enough energy is put in the supershells can break open, allowing the hot gas to flow upwards into the halo, like a chimney. The denser, swept up ambient gas is also raised to large heights above the plane.

Molecular clouds are the coldest, densest ISM structures and it may be difficult to raise them far from the disk by the chimney process. Alternatively, molecular clouds could form out of warmer clouds as they cool and return to the disk as part of the cycle. For comparison, the gases usually observed above the plane have a very low number density of .1 to 1 cm^{-3} , while molecular hydrogen has a density of 10^2 to 10^3 cm^{-3} .

Figure 1 shows this model. The shaded regions are hot gas rising, with the chimney walls being represented by the solid lines. The circles are clouds that have formed in the hot gas and are sinking back down into the disk. The gas is thus believed to be multi-phase, and as mentioned above, has been observed to be so.

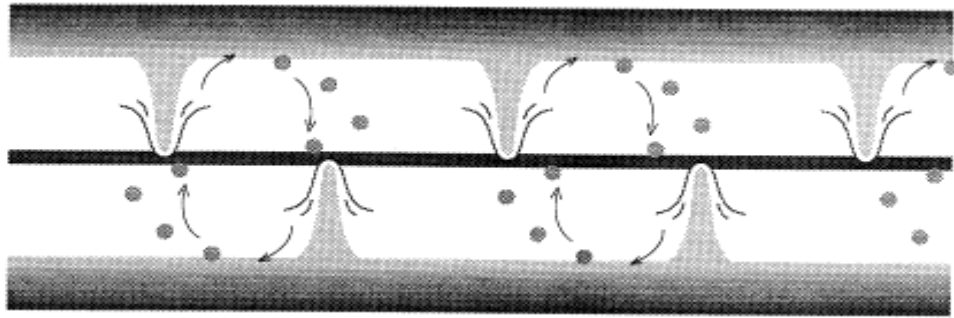


Figure 1: From model of the disk-halo cycle. The shaded areas are hot gas rising, and the circles are gas clouds that have formed and are sinking back to the disk. Chimneys are represented by the solid lines. Norman & Ikeuchi (1989).

1.2 NGC 891

Looking at a nearby, external edge-on galaxy gives us an excellent view of the disk and halo. From inside of the Milky Way, it is difficult to discern the distances to objects outside of the plane, such as gas clouds. Objects outside of the plane may not simply be rotating around the center of the Milky Way; they may have motions in the vertical or radial direction, making it difficult to infer a distance simply from the Doppler shift, as can be done in the disk. Edge-on galaxies, on the other hand, give a very clear look at the vertical structure. The spiral galaxy NGC 891 is the best studied edge on galaxy. Its basic properties are very similar to the Milky Way, and this has led astronomers to consider it a near twin of our own galaxy. At a distance of 9.6 Mpc, this galaxy is almost perfectly edge on, and affords us the chance to study its vertical structure. In the halo of NGC 891, almost every component of the ISM has been detected, except for molecular gas.

Howk & Savage (1997) took deep optical images of NGC 891 using the WIYN 3.5 m telescope. They noticed that there was extinction high (up to 2 kpc) off the plane of the disk. This extinction can be seen in Figure 2; note the dim, patchy regions above the main absorbing disk. The amount of extinction seen in the optical images is able to be turned into a column density of dust.



Figure 2: Optical image of NGC 891. The extinction regions that are of interest lie off of the plane of the galaxy, and are dim and patchy. Image courtesy of J. C. Howk

Following a few assumptions, extinction can also be turned into a column density of gas. The first assumption is that dust is similar in NGC 891 to the dust seen in the Milky Way. When light from a star passes through a dust cloud, it becomes scattered and absorbed. If the wavelength is on order of the size of the dust particles, it can be become blocked or scattered. Only those rays missing the particles get through. Of course, if the wavelength is much larger than the particles, than they pass through unaffected; the shorter wavelengths are more likely to

be preferentially removed. Observers along a line of sight see a reddened source, while observers on other sides see scattered light rays that are bluer (Carroll & Ostlie 2007). Using this method, Howk and Savage were able to show that the dust reddened the light in roughly the same way as Milky Way dust.

The second assumption is that the dust to gas ratio is the same in NGC 891 as it is in the Milky Way. One other assumption that has to be made is the relative distribution of dust and gas along a line of sight; Howk and Savage assumed that some fraction of light, x , is emitted in front of the dust. We define the optical depth, and then apply these assumptions. The optical depth is how much light is attenuated by a column of material; it gives how dense and thick a gas cloud is. It is useful because it is related to the column density of absorbing material, N , the observed intensity and the intensity incident on the cloud. By viewing the dust feature through the different filters, they could constrain a ratio of reddening to extinction and the value of x . Then, finding the optical depth and column density is relatively easy (Carroll & Ostlie 2007). The equation for the optical depth is

$$\tau_{\lambda} = \int n_d(s') \sigma_{\lambda} ds' = \sigma_{\lambda} N_d$$

τ_{λ} = optical depth for our wavelength
 n_d = number density of scattering particles
 σ_{λ} = scattering cross section along line of sight
 N_d = column density

The form of original intensity, based on the Howk and Savage assumptions, is

$$I_{\lambda} = (1-x)I_{\lambda,o} e^{-\tau_{\lambda}} + xI_{\lambda,o}$$

I_{λ} = intensity observed
 $I_{\lambda,o}$ = intensity emitted from source
 x = fraction of gas not affected by extinction

Once the column density for a feature is found here, it is possible to multiply it by the area, which gives a total number of atoms. This can then be converted into a mass with helium corrections applied, since the gas is a mixture of mostly hydrogen and helium. Using this process, Howk found that the column density of a typical feature was $N(\text{H}) \geq 10^{20} \text{ cm}^{-2}$, which implied masses of $4 \times 10^4 - 10^6 M_{\text{sun}}$ (Howk 2005). The only question remaining is the type of gas that is associated with the extinction in NGC 891. The extinction is very patchy, with typical sizes around a few arcseconds. Some of the gas associated with this extinction may be molecular. Most of the gas in the ISM is either molecular or atomic. Vertically extended atomic gas is known to exist, but has not been observed with sufficient angular resolution to look for a correlation with the extinction patches.

As far as molecular gas is concerned, there are competing claims from Garcia-Burillo et al. (1992) and Scoville et al. (1993). Molecular gas is most easily traced by CO emission as the emission from molecular hydrogen is extremely weak. Garcia-Burillo et al. claimed to find CO gas extended at heights of 1-2 kpc off the plane of the NGC 891, using the Instituto de Radio Astronomía Milimétrica (IRAM) telescope, a 30-m single dish in Spain. Scoville et al. used the Owens Valley interferometer, and did not find any of the extraplanar gas. It is hoped that the new, more sensitive Combined Array for Research in Millimeter-wave Astronomy (CARMA) will be able to detect these molecular clouds off the disk. The goal is to search off the plane of NGC 891 using the CARMA array for molecular gas, which may correlate with the extinction patches observed.

2. Interferometry:

Radio astronomy has many advantages over the other types of observing. For one, radio waves are long, which means they are less likely to be scattered or absorbed by particles in space and in the atmosphere. Two, radio arrays can be used to create an interferometer; the result is that a telescope array of size D achieves the same resolution as a single telescope of diameter D . The resolution limit is proportional to λ/D . Also, some astronomical objects are most easily observed in the radio. Radio waves are created in a number of ways, and so it is possible to use their emission to measure physical processes and properties, such as the temperature, density, or even motion of atomic and molecular clouds.

Much of the following discussion is adapted from Gary (2005). Radio interferometry works in similar fashion to normal interference seen from double slit experiments. An interferometer is most easily understood by simply looking at one baseline, and then applying the concepts to the entire array. In this case we have two radio dishes separated by a distance, which is called a baseline. If these two telescopes are pointed at the same point source, the result is constructive and destructive interference, depending on the relative path length or optical path length, in units of wavelength, from the source to the two telescopes, which is also dependent on the direction of the source. Thus, the interfered signal contains information about the spatial distribution of emission on the sky, as seen in figure 3.

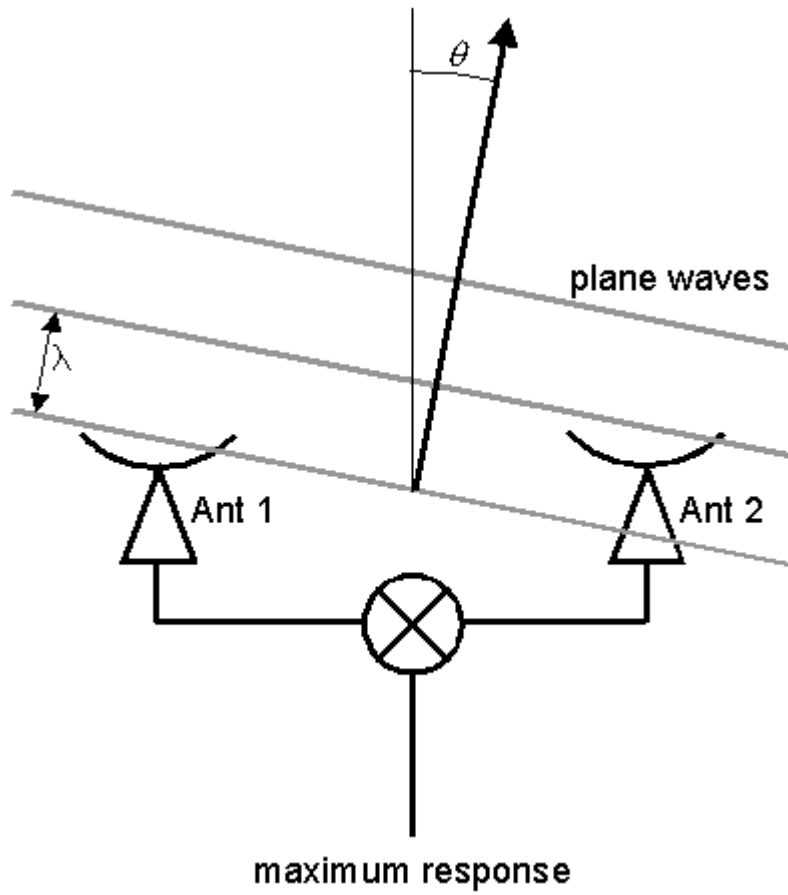


Figure 3: A point source that is not directly overhead creates a path difference between two antennae. Gary (2005)

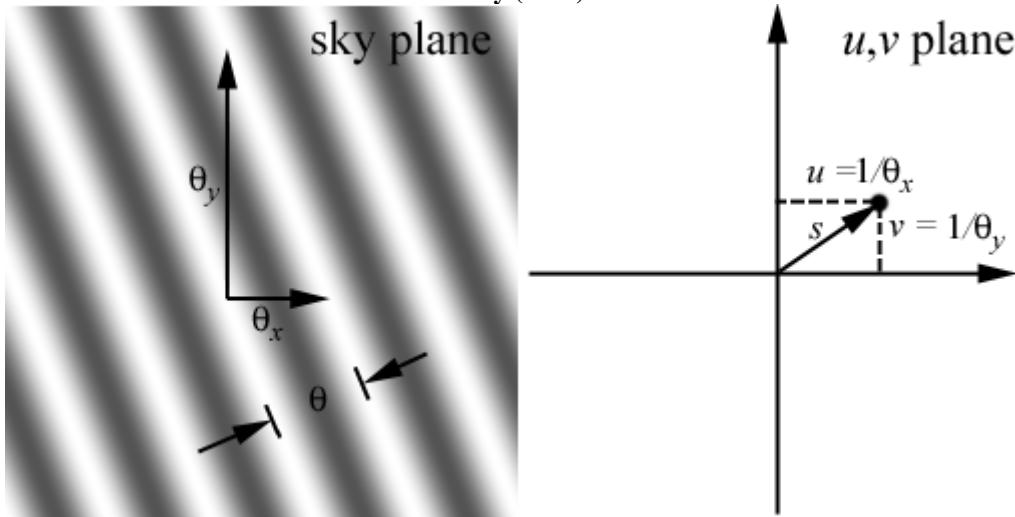


Figure 4: The path difference from a source leads familiar fringe patterns. Gary (2005)

When looking at a point source, the interferometer measures a phase depending on the path length difference, which depends on the angular orientation. As seen in Figure 4 the path length difference leads to a familiar fringe pattern, with each fringe separated by an angle θ . If a point source is located at an angular distance θ_1 , then an interferometer will measure the x and y components of the phase at an angle ϕ , where $\phi=2\pi \theta_1/ \theta$. The length of this vector is equal to the amplitude of the point source. This can be better seen in figure 5.

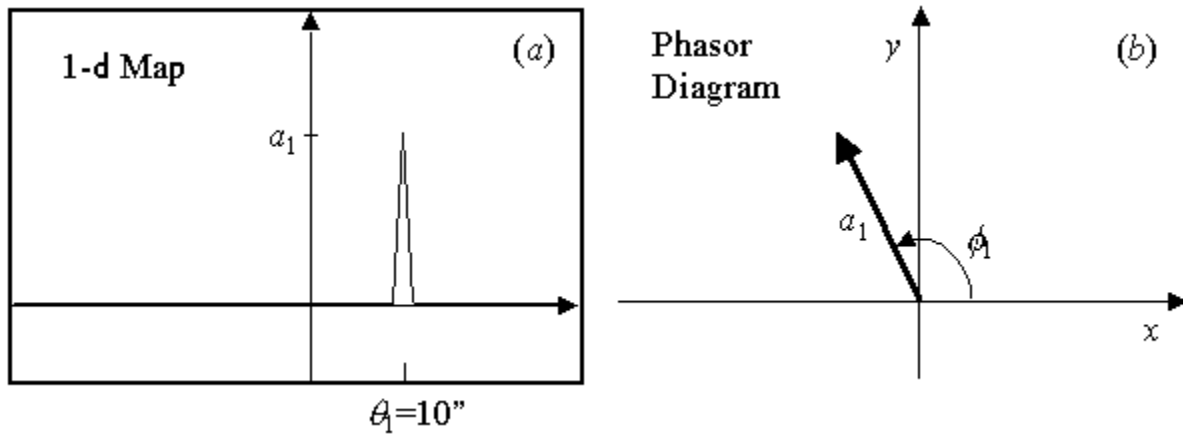


Figure 5: The position of the source corresponds to a phase, seen by the phase diagram on the right. Gary (2005)

If there are two point sources, then two sharp peaks present themselves in the intensity map, and the resultant becomes the vector sum of the two point sources.

$$a_r e^{i\phi_r} = a_1 e^{i2\pi\theta_1/\theta} + a_2 e^{i2\pi\theta_2/\theta}$$

A continuous distribution is treated as a large number, N , of point sources. This means that the resultant is going to be the sum of the N complex numbers.

$$a_r e^{i\phi_r} = \sum_n a_i e^{i2\pi\theta_n/\theta}$$

We can actually convert this form into our coordinate system. Figure 4 shows the spatial frequencies on the sky, (u, v) ; these belong to the plane of the array that has been projected into

the direction of the source. They are x-y coordinates for this plane, related by $u=x/\lambda$ and $v=y/\lambda$, and are components of s , the fringe spacing. s is inversely proportional to θ , meaning that smaller fringe spacing is equal to a larger angular scale on the source. θ also has components (l, m) , which are the angular coordinates on the sky plane in the east and north directions. This coordinate system belongs to a plane that is perpendicular to the source direction. The equations describing the amplitude and phase relationship become

$$a_r e^{i\phi_r} = \sum_n a_i e^{i2\pi(ul+vm)}$$

Now, we define the continuous function $V(u,v)$, the visibility function, and say that it is equal to $a_i e^{i\phi}$. We also define a sky brightness function, $I(l, m)$, which is the continuous equivalent of a_i in the above equation. $V(u, v)$ is the Fourier transform of $I(l, m)$. If we generalize the above discrete sum into an integral over all space, we then find that

$$V(u, v) = \int I(l, m) e^{-i2\pi(ul+vm)} dl dm$$

$$I(l, m) = \int V(u, v) e^{i2\pi(ul+vm)} du dv$$

These functions will also contain noise from the system. Our baselines only sample points of V , instead of all of V , and this is called our sampling function, $S(u, v)$, as will be discussed further below. The Fourier-transform of $S(u, v)$ is called the dirty beam, $B(l, m)$; it represents the diffraction pattern, and actually distorts the data. The data received is actually the product of the sampling function and the visibility function, and so the image becomes the convolution of the brightness function and the beam function. When we transform this back to the brightness function, we now have what is called the “dirty” image, given by

$$I_D(l, m) = \int S(u, v) V(u, v) e^{i2\pi(ul+vm)} du dv$$

An image description of all of these various functions can be seen in figure 6.

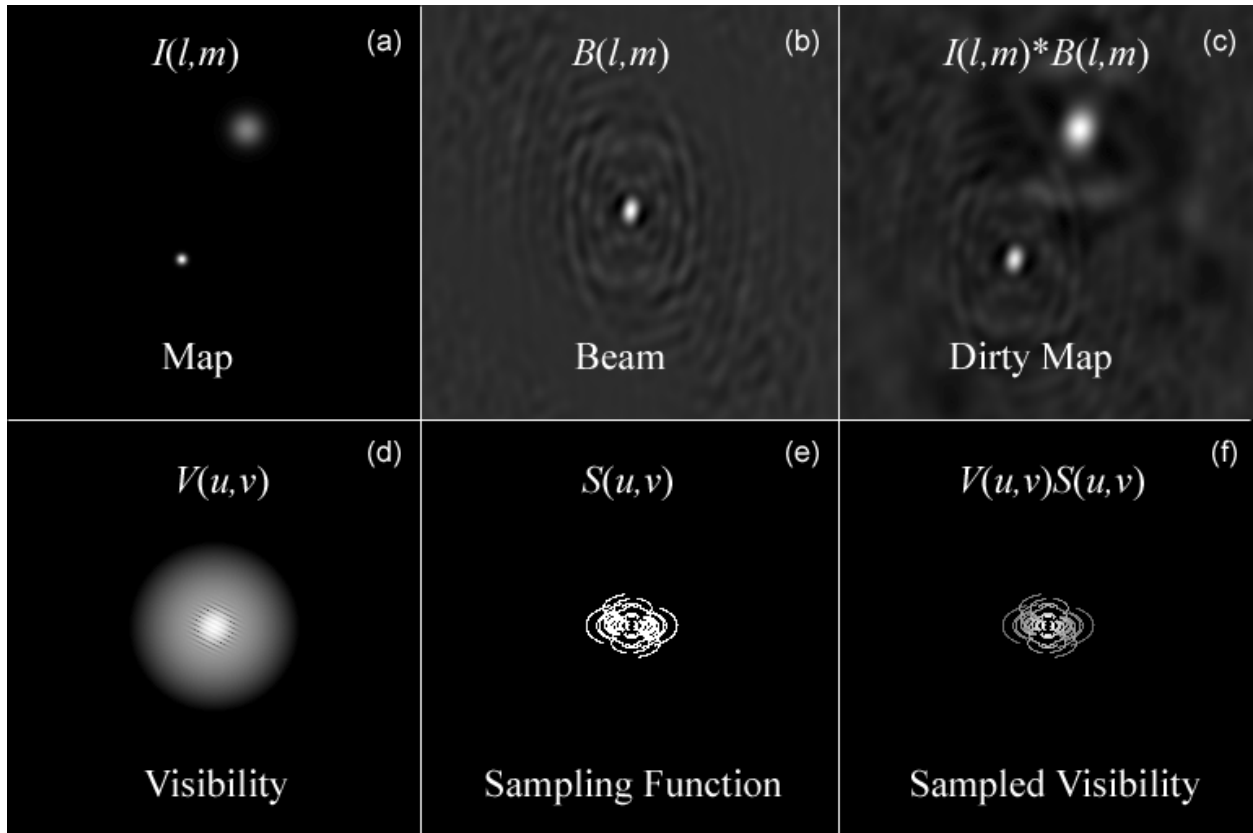


Figure 6: This figure is a pictorial description of the different functions. Starting top left, $I(l,m)$ is the sky brightness function, $B(l,m)$ is the dirty beam, and last is the convolved image. On the bottom row, $V(u,v)$ is the visibility function, and $S(u,v)$ is the sampling function, which only samples part of V . The last image is the product of V and S . Gary (2005)

Radio astronomy is inherently limited due to the sampling. We may treat our array of dishes like a full aperture telescope, but in reality we only have pieces of the full aperture. A single baseline at a specific time gives position information only on the angular scale λ/D , where D is the projected baseline length perpendicular to the source; this information is only in the direction of the baseline vector. In order to have a “filled” aperture, several baselines are needed to fill in the various angular scales. By letting the Earth rotate, many more orientations are achieved. Figure 7 is an example of our sampled aperture from a ten-hour observation. The dark dashes are where we have data points, and the rest of the blank areas are empty.

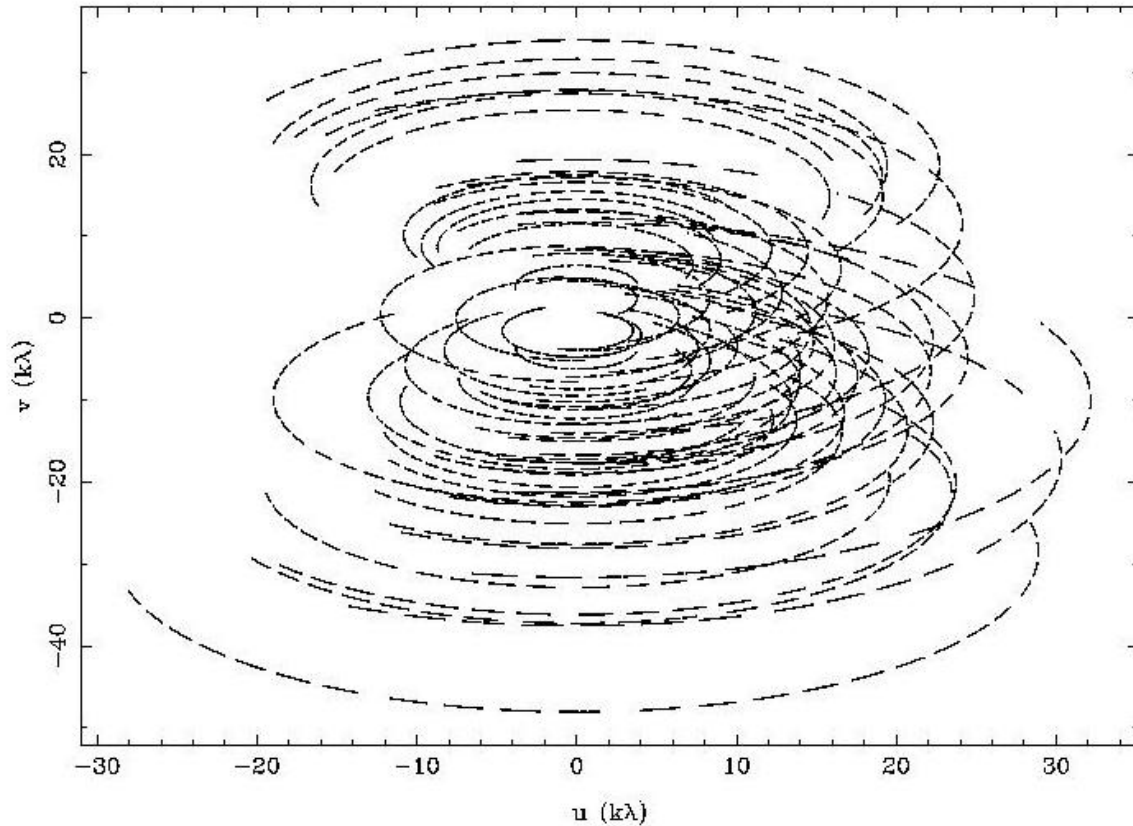


Figure 7: An image representation of our sampled aperture from a full track, taken over a ten hour period. The dashed lines are areas for which we have data.

In order to have an accurate representation of the sky, the dirty beam needs to be removed. This seems like it could be an easy process, but our sampling function actually limits the process. Figure 8 shows a simple example of the relationship between an aperture and its Fourier Transform.

Fourier Transform relationship of aperture and beam

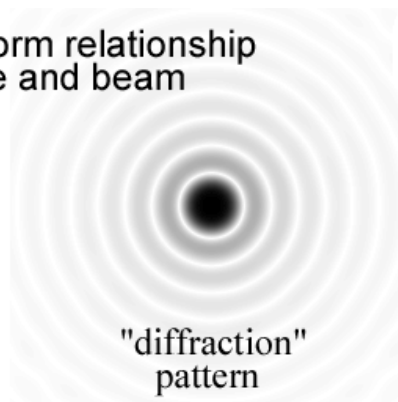


Figure 8: This image shows the relationship between a perfect aperture and its Fourier transform; the airy disk on the right contains sidelobes that complicate the deconvolution process. Our beam actually has worse sidelobes. Gary 2005

For a perfect circular aperture, the Fourier transform is the airy disk seen above. The airy disk contains sidelobes, and in a 2D plot the difference between a Gaussian and our airy disk, as seen in figure 8, the difference more easily seen. However, note that our sidelobes are much worse because we only have a partially filled aperture, making the process of deconvolution more complicated.

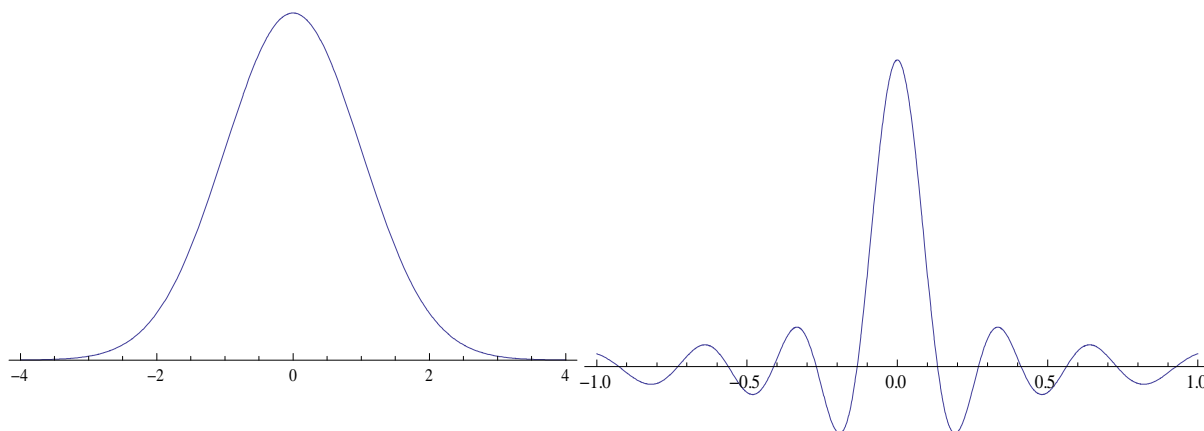


Figure 9: For a perfect aperture, the 2-D plot looks like a Gaussian. The airy disk has sidelobes like those seen on the right, complicating the deconvolution process. Created using Mathematica 6.0

It is no longer a simple method of directly deconvolving the dirty beam, if we knew it, because we now have zero crossings. There is also noise in the u-v data, which is also problematic to deconvolve. The most common method to deconvolve the image from the dirty beam is CLEAN.

2.1 Clean

Clean is an iterative process that has been developed to remove sidelobes from the dirty images. It treats the radio source as a number of point sources, and works on each point individually. There are many different ways to clean an image, and even these different methods have their own variations. We used a variation known as Steer, Dewdney and Ito (SDI) clean. Essentially the program identifies the brightest point in the dirty image. It assumes that no side lobes from other emission distort this point. A small (~5-10%) fraction of the dirty beam centered at this point is subtracted off from the entire image, and the process is repeated. Eventually the point becomes dimmer than the rest, and then the process works on the next brightest point. The process works down until about the noise level of the image, at which time the side lobes are removed, and the image is “cleaned.”

3. Observations

We used the Combined Array for Research in Millimeter-wave Astronomy (CARMA) to collect our data. This array consists of fifteen telescopes, and is the combination of two older arrays: the Berkeley-Illinois Maryland Association (BIMA) array, and the Owens Valley Millimeter Interferometer. There are nine 6.1 m dishes from the BIMA array, and six 10.4 m dishes from the Owens Valley array, creating 105 baselines. The combination of these two arrays has created the most powerful millimeter array of today, with a combination area of 772 square meters. These two arrays were combined one and a half years ago.

The CARMA array is located on a flat plateau at 7200 feet about sea level in eastern California. This elevation greatly reduces the amount of water vapor in the atmosphere. The wavelengths that we are observing are easily absorbed by the water vapor, and so this elevation is a great advantage for viewing. The CARMA array has resolution capability of 0.1" at 230 GHz (in the A array). It observes at 3mm (85-116 GHz) and 1mm (215-270 GHz) wavelength, which covers many of the lowest rotational transitions of brightly emitting molecules. Our data were taken in the D array, with dishes 11-150 m apart. Since any emission from molecular hydrogen is very weak, we are using CO as a tracer gas, and are observing the lowest rotational transition of CO (CO 1-0). This occurs at a wavelength of 2.6 mm (or a frequency of 115.271 GHz); the result is an angular resolution of 5".

4. Reduction

Our data consisted of eighteen tracks, a mixture of partial (only a couple of hours long) and full tracks (about ten hours long). The tracks were taken over the months from March to July of 2007. Before being able to transform our data from the Fourier image domain to the image domain we have to calibrate it. Calibration compensates for errors from the telescopes themselves, any electronic errors, any position errors on the sky or in the array itself, and any atmospheric changes due to turbulence and weather. Before beginning any calibrations, some routine automated flagging of bad data is done.

The first calibration is simply to check that all of the antennas positions are correct. This is done by observing a large number of bright point sources spread over the sky, and is usually done right after the antennas are moved a new configuration. This is done by the observing facility, and the data is provided to us. Point sources are used because the amplitude is expected

to be constant, and the phase constant, which makes them useful for calibration. Any deviations from these are believed to be from the antennas, atmosphere or electronics.

Next we calibrate phase and amplitude errors as a function of time using the bright point source 3C84, which we observe every half hour. The correction factors are known as complex gains and are complex numbers. This is actually two processes: the flux calibration and the gain calibration. The flux calibration is based on an observation of a planet during the track; planets have well measured fluxes. However, planets are not point sources with zero flux, and this reduces the visibility; this can be corrected for, and planets are used to create a flux scale, which provides the overall amplitude scale for the gain calibration. The gain calibration is a phase and amplitude vs. time calibration, and so we need to calibrate the phase; for this we use a point source, 3c84.

In general, the center of a galaxy can be considered to be a point source and all of the other “point” sources, i.e., the rest of the galaxy, have a phase difference between two telescopes. These relative phase differences also depend on time; this is due mainly to turbulence in the atmosphere. In order to calibrate the data, we observe 3c84, and demand that it has zero phase. There is some error in this method, since the point source and galaxy are viewed at different times and at different places through the atmosphere. To compensate for this, we measure the point source every thirty minutes, and we pick a source close to the galaxy. Both of these changes are then applied through the gain calibration; during this calibration we demand that the measured signal from 3c84 has the same flux found during the flux calibration, and we force the phase to be constant (or zero). The corrections found for 3c84 are then applied to NGC 891.

Next is the passband calibration. The spectrum is made with a correlator, which introduces noise, and can create different amplitudes and phases due to electronic errors. This

introduces amplitude and phase variations across the passband. This calibration requires a sufficiently bright source; for us, this happened to be the same as our phase calibrator, 3c84. This process takes the point source, and forces the amplitudes to be constant and phases to be zero across the passband. Then these changes are applied to the galaxy.

After all of these steps, we have a calibrated dataset for the galaxy; there is more editing to be done to the galaxy data. This involves looking at each spectrum for any bad channels or data that did not get flagged in the initial calibration. After this, we can transform our u-v data, and create our dirty map. The UV data is combined and then transformed into one map; this reduces the amount of intrinsic noise. Then we apply the process of clean, and achieve one cleaned map. For our data, we used tracks one, two, thirteen, seventeen and eighteen. These were the longer and cleaner looking tracks, and the missing tracks should not add much to the signal. Also, some of the missing tracks had calibration problems.

5. Results

If we sum over all of the velocity channels of our cleaned cube, we create a zeroth-moment map, which is a total intensity map with Right Ascension (RA) and Declination (Dec) axes. From this we are able to determine the column density of the molecular gas in the galaxy. We start by finding the brightness temperature, the temperature a blackbody would have to have in order to duplicate an observed intensity at a specific frequency. This temperature can be related to the column density along our line of sight. We can find this by the following equation:

$$\frac{S}{\Omega_A} = \frac{2kT_B}{\lambda^2}$$

S=flux density in $\text{ergs}^{-1} \text{cm}^{-2} \text{Hz}^{-1}$

$$\Omega_A = \frac{2}{8 \ln(2) a'' x b''} \left(\frac{1}{206,265} \right)^2$$

λ =wavelength in cm

k=Boltzmann constant in cgs units

T_B =Brightness temperature in Kelvin

The $a'' \times b''$ are the dimensions of the dirty beam in arcseconds. We also convert S into Janskys/beam. One Jansky or Jy is a unit of flux equal to $10^{-23} \text{ ergs}^{-1} \text{ cm}^{-2} \text{ Hz}^{-1}$ and is the unit used in our maps. For the case $\lambda=2.6 \text{ mm}$, our brightness temperature becomes

$$\frac{T_B (K)}{S (\text{Jy} / \text{beam})} = \frac{92.3}{a'' x b''}$$

A way to find the column density is by the “x-factor.” The x-factor applies to the Milky Way, but because NGC 891 is assumed to be our twin, it is assumed to be the same. It has been found for the Milky Way that there is a correlation between an observed intensity and a column density of molecular gas. This was done by assuming that the clouds are in equilibrium; from this it is possible to derive the mass from the width of the emission and from the size of the cloud (Scoville & Young 1991). The result, uncertain by a factor of two, is $x=3 \times 10^{20} \text{ mol cm}^{-2} / \text{K km s}^{-1}$, which includes the mass of helium as a correction, and with a few conversions, can be rewritten as

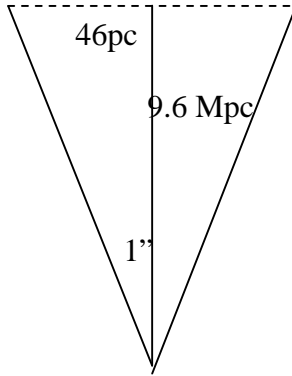
$$x = \frac{591 M_{\text{sun}} \text{ pc}^{-2}}{a'' x b''} / \frac{\text{Jy km}}{\text{beam s}}$$

A similar result was found from diffuse gamma ray emission in the Milky Way. When cosmic rays run into clouds of H_2 , a gamma ray and pion are emitted. The intensity of gamma rays depends on the mass of gas present.

By using the above methods for the Milky Way, we can apply them to NGC 891 allowing us to find the mass and thickness of any clouds detected off the disk; if we do not find them, we can set a limit on their masses based on the noise in our map. We start with equation above

$$1Jy \text{ km s}^{-1} = \frac{591}{a'' \times b''} M_{Sun} \frac{beam}{pc^2}$$

Since we are trying to find the amount of mass per beam, we need to find the number of parsecs per beam. This is accomplished by taking the distance to the galaxy, and finding the distance subtended by 1 arcsecond. In our case, since the distance away is 9.6 Mpc, we find that there are 46 pc/arcsecond.



If we square this value, we can multiply it by the beam area, which we approximate to be a rounded beam of 3.9''x3.9''. This will give us a result in pc²/beam. Now we can multiply this result by the above equation to find the mass of the clouds.

$$9.6 \text{ Mpc} \tan 1'' = 46 \text{ pc/arcsec}$$

$$46^2 \times \frac{3.9'' \times 3.9''}{beam} = 3.2 \times 10^4 \frac{pc^2}{beam}$$

$$\begin{aligned} 1Jy \text{ km s}^{-1} &= \frac{591}{a'' \times b''} M_{Sun} \frac{beam}{pc^2} \times 3.2 \times 10^4 \frac{pc^2}{beam} \\ &= 1.2 \times 10^6 M_{Sun} \end{aligned}$$

Of course, the real question is the whether or not we found any signs of molecular hydrogen associated with the extinction patches off the plane. Following are several images from our data. Figures 10, 11, and 12 contain small images that progress in observed velocity. As can be seen the galaxy moves in through the frame on the upper left, and out of the frame through the bottom right. Contours are plotted over top of the black and white image, giving an idea of the noise level, and any real emission that may be present. Figures 13 and 14 are the zeroth-moment maps, and show up close what we are observing. Figure 13 shows only positive emission values for our data, while figure 14 shows the negative values as well. These contours are plotted over the Howk and Savage optical image of NGC891 which has been processed to remove smoothly distributed emission and reveal small-scale structure.

The regions of interest are any patchy extinction regions off of the plane of the galaxy; we are looking for any areas where we have any putative real detection that matches up with these areas. We require that any real emission would be about five times the rms noise; for the moment map, this value was $2.5 \text{ Jy beam}^{-1} \text{ km s}^{-1}$. If we multiply this value by our above constant of $1.2 \times 10^6 M_{\text{sun}}$ we find that we could have detected as little as $3 \times 10^6 M_{\text{sun}}$. Howk and Savage estimated that the amount of gas in the clouds would be on order $4 \times 10^4 - 10^6 M_{\text{sun}}$, a limit that we have not quite reached. As can be seen from figure 12, we did not observe any gas clouds extended off of the plane. The areas that overlap the extinction are noise, and not actual emission. Figure 13 shows negative noise overlapping some of these areas, but unfortunately, negative noise is not real emission. Therefore, we have to conclude that we did not detect CO emission, and therefore did not find any molecular hydrogen off of the plane of NGC891.

We are also able to find the vertical thickness of the main layer. From our zeroth-map we created an average vertical profile from which we printed values and read off the full width half

maximum (FWHM). This value was approximately 6.5 pixels; since we chose one pixel to be equal to arcsecond, this means the FWHM is approximately 6.5". The beam FWHM is approximated to 3.9", which means that the layer is resolved. From these two values we find that the deconvolved thickness is 5.2". We already found above that there are 46 pc/arcsecond, and so by multiplying these results with the beam's FWHM, we conclude that the thickness of our layer is 300 pc. This is close to 276 pc, the value that Scoville et al found in their paper.

6. Conclusion

We observed NGC891 over the course of several months using the CARMA array. The first important result was that we were unable to detect any molecular gas extended off of the plane of the galaxy. We found that our array had a mass detection limit of about $3 \times 10^6 M_{\text{sun}}$, while the predicted mass of the clouds were $4 \times 10^4 - 10^6 M_{\text{sun}}$; this is somewhat below our detection limit. We were also able to discern the thickness of the molecular layer of NGC891 to be about 300 pc, which is close to other observed values.

There are a few reasons as to why we were unable to detect any molecular gas extended off of the plane. The foremost reason is that the predicted masses of the clouds are at the limit of our sensitivity. Our sensitivity may also not have been nearly as good as we predicted; the tracks were noisy, and not as good as predicted. There were also a few assumptions that were underlying the prediction of the masses of the molecular clouds, and it is possible that these are wrong; the dust in Milky Way and the x factor for the Milky Way could possibly not apply to NGC 891, though we do not believe this to be true. There is also some uncertainty in the value of the x-factor, and this could also play a role.

It is possible that the other tracks excluded from the final map could help improve the noise and resolution limits, but in general they should not affect the result by much. We have to

conclude that if the molecular gas exists off of the plane, then it is beyond our sensitivity limits for the time being, and we will have to wait until a more powerful millimeter array is built.

Thanks to Dr. Rand for his time and patience, and a special thanks to Tom Hess who helped us battle Linux every step of the way.

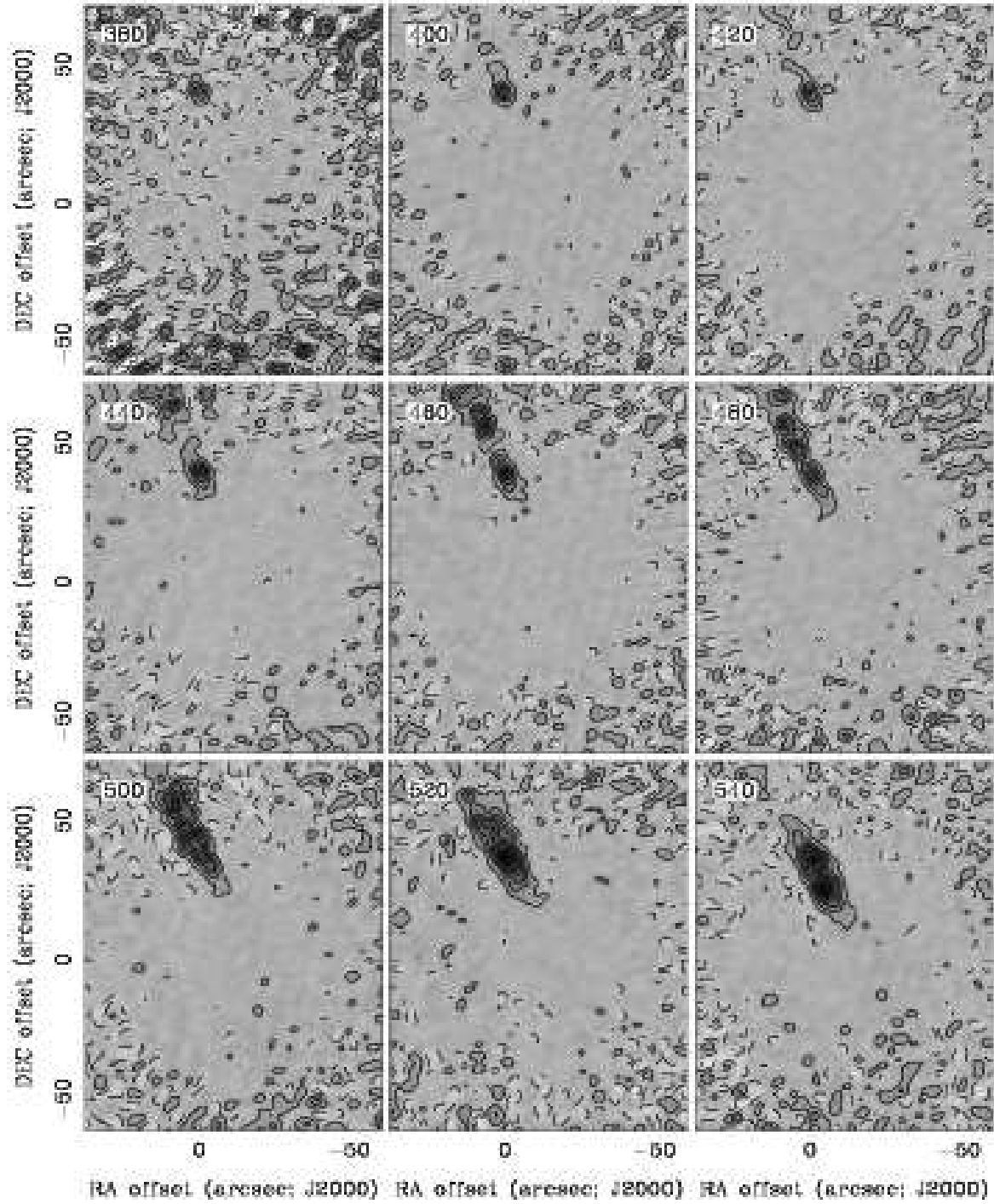


Figure 10: The first set of channel maps. These show the track as it progresses in velocity. The galaxy moves across the images from the top left to the bottom right. The contours are in units of Jy/beam of ± 3 , ± 9 , ± 15 , ± 21 , ± 27 , ± 33 times the noise.

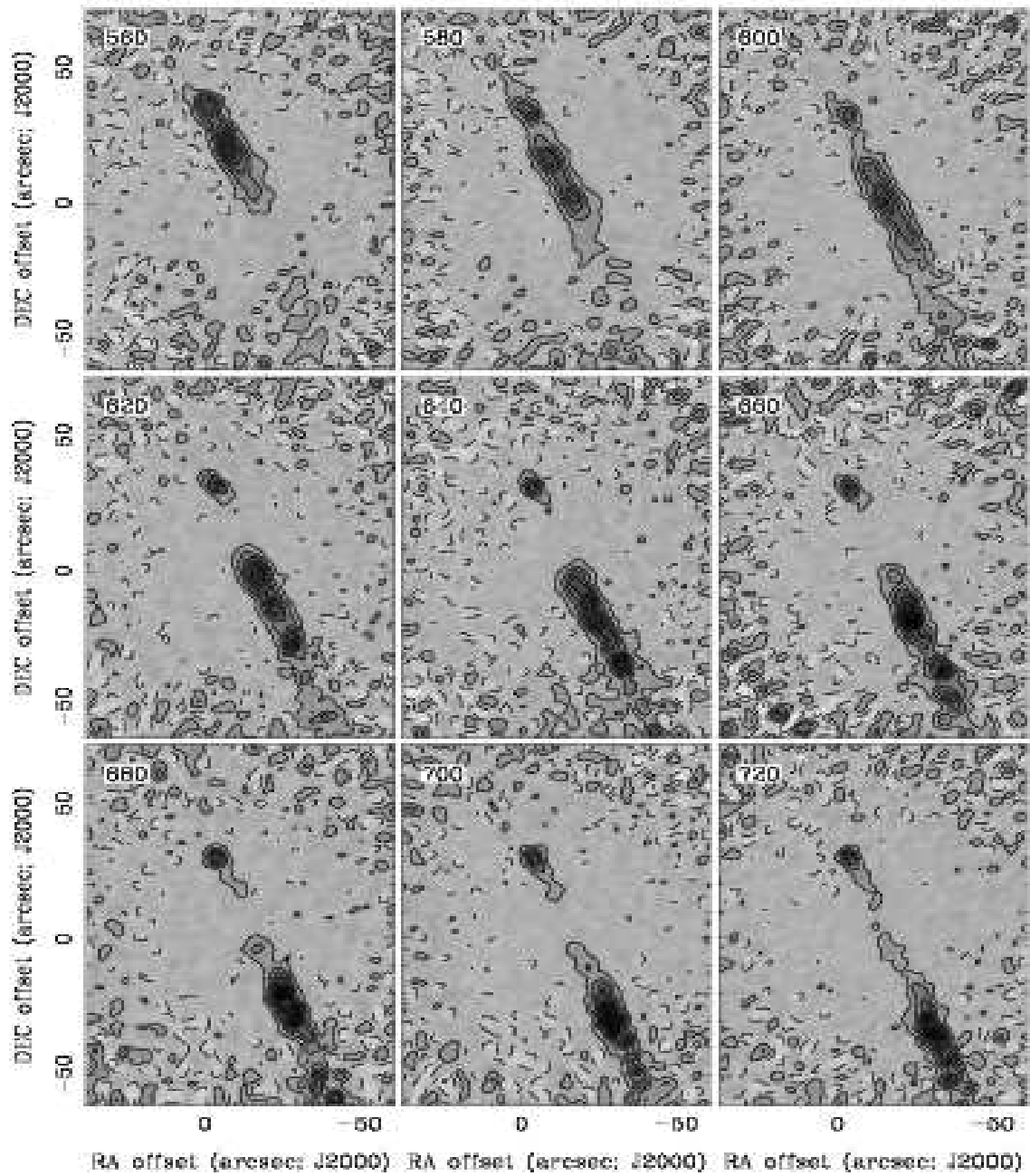


Figure 11

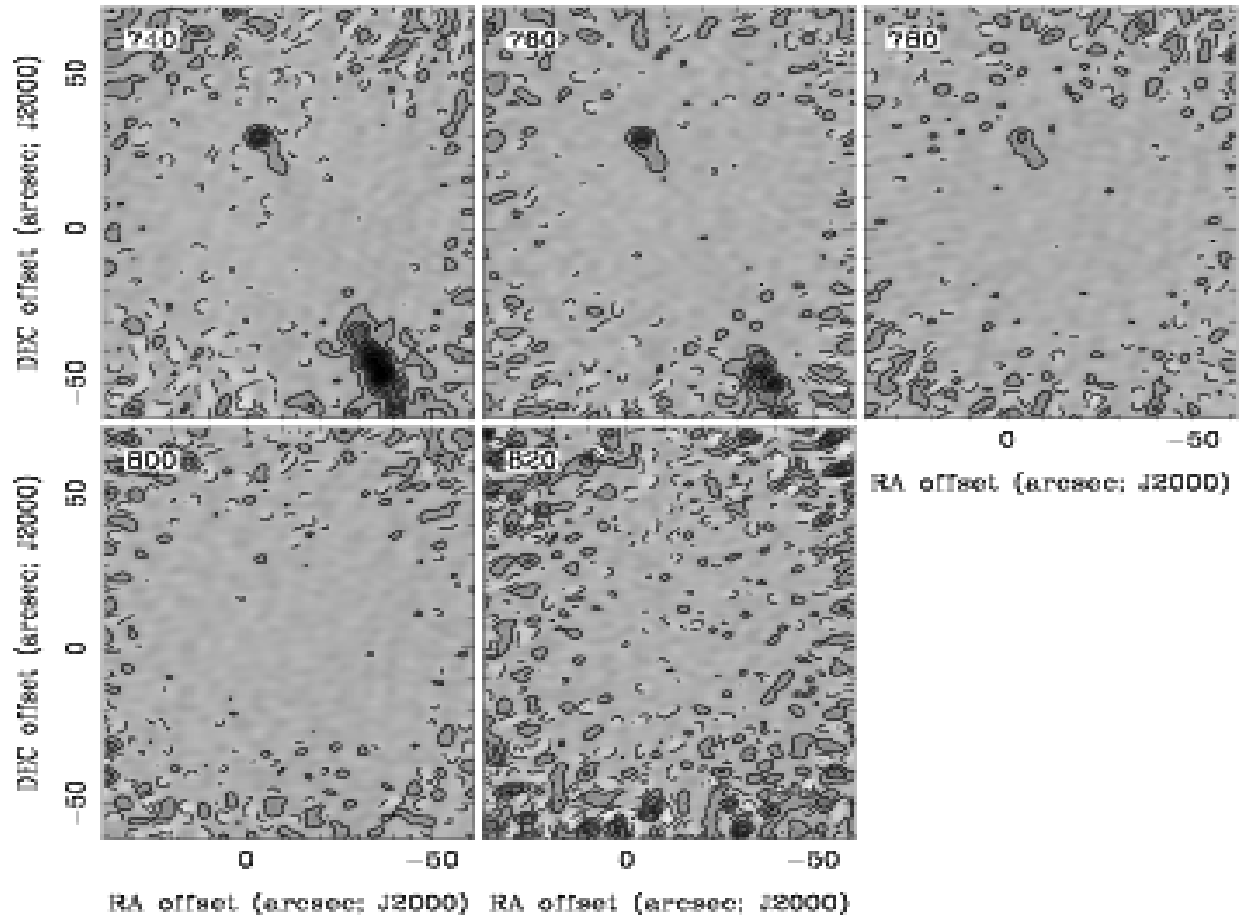


Figure 12

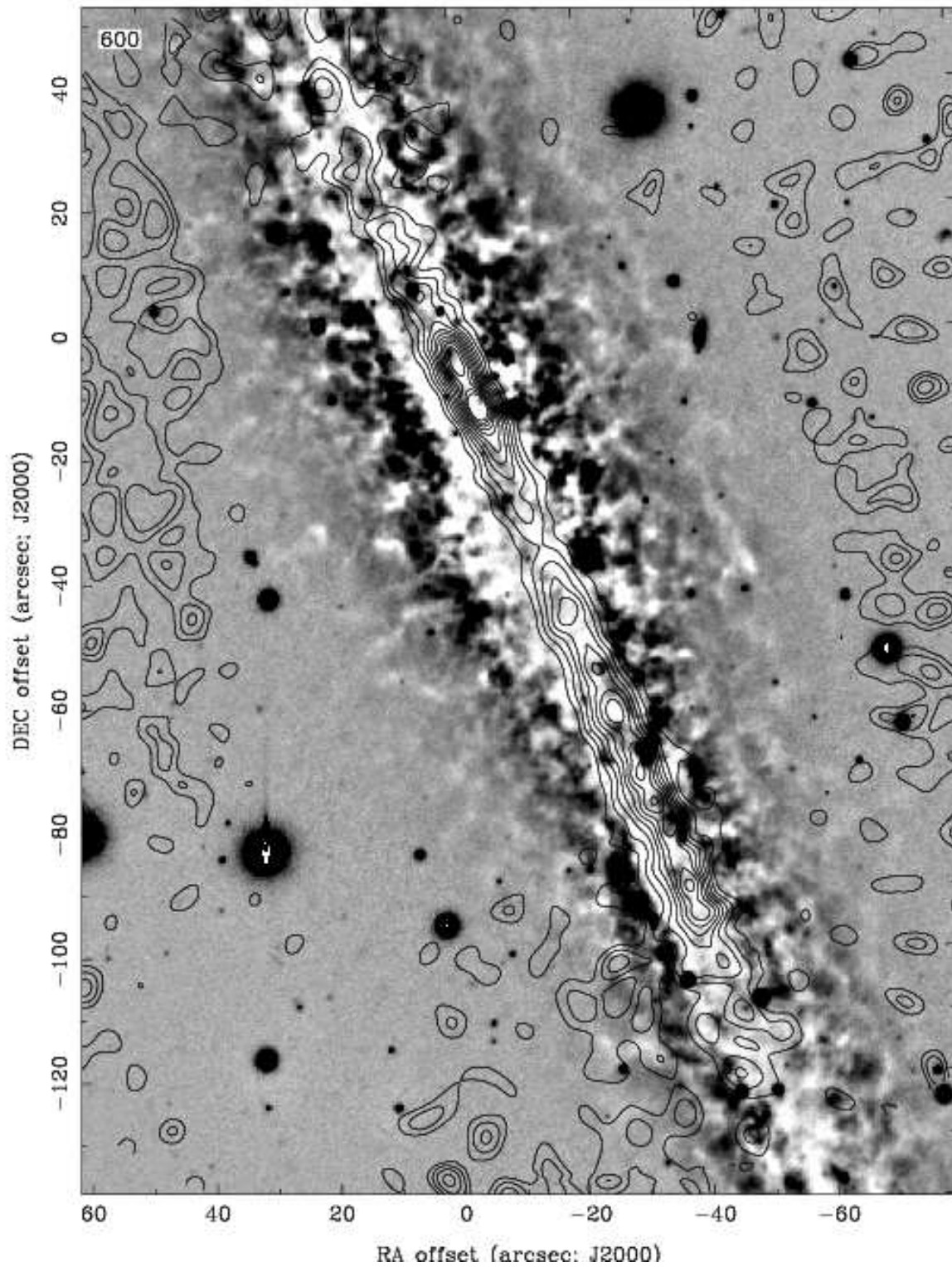


Figure 13: Processed optical image of NGC 891 revealing dust features from Hawk & Savage (1997), with contours of CO emission overlaid. The contours are in units of Jy/beam km/s of 50,100,150,200,250,300,350,400,450,500,550 times the noise at the map center.

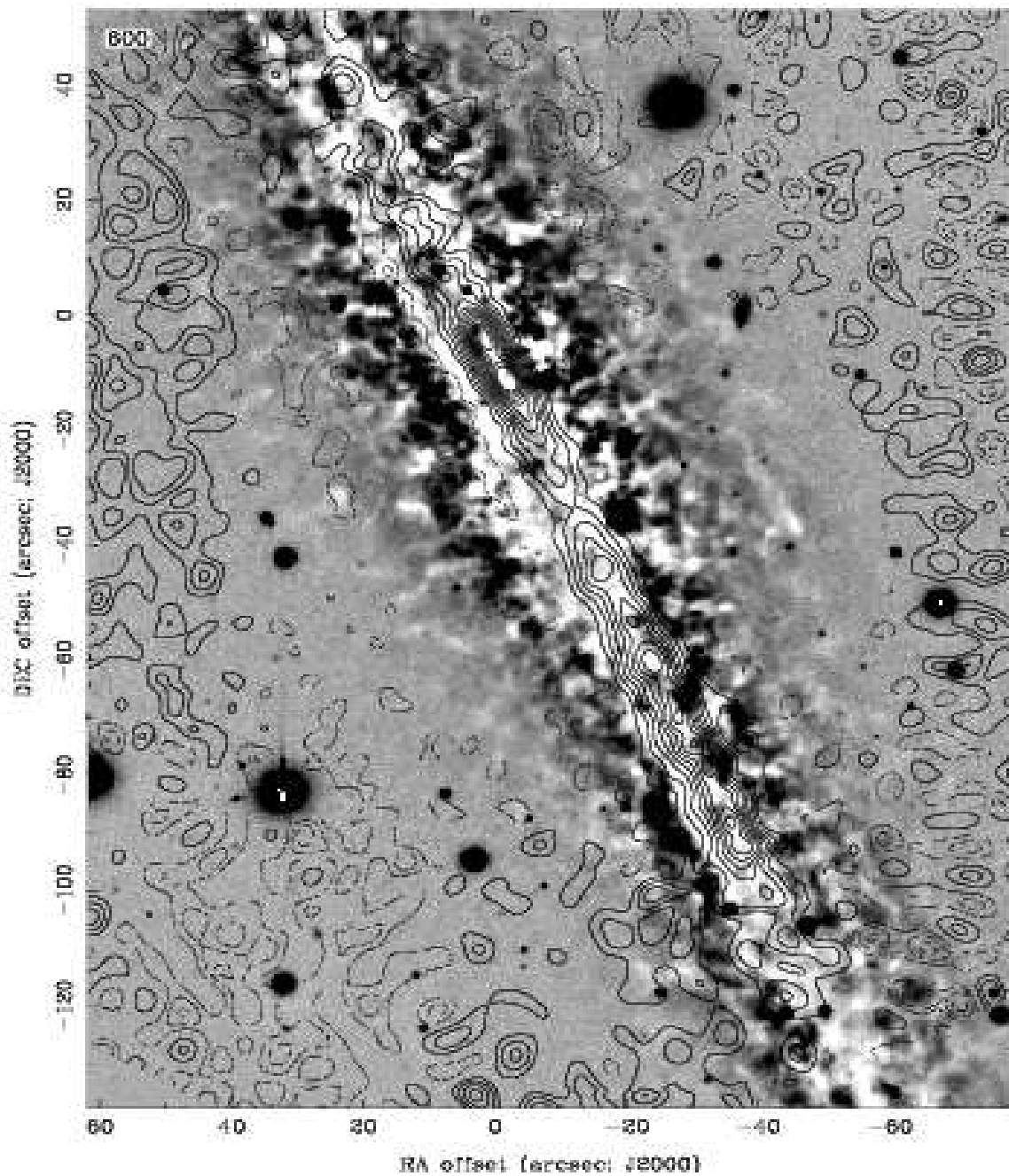


Figure 14: Processed optical image of NGC 891 revealing dust features from Hawk & Savage (1997), with contours of CO emission overlaid. The contours are in units of Jy/beam of ± 50 , ± 100 , ± 150 , ± 200 , ± 250 , ± 300 , ± 350 , ± 400 , ± 450 , ± 500 , ± 550 times the noise.

Carroll, B.W. & Ostlie, D. A., *Introduction to Astrophysics*, 2007

Gary, D. 2005, <http://web.njit.edu/~gary/728>

Garcia-Burillo, S., Guélin, M, Cernicharo, J., & Dahlem, M. 1992, *A&A*, 266, 21

Howk, J.C., 2005, *Astronomical Society of the Pacific Conference Series*, **331**, 287

Howk, J. C., and Savage, B. D. 1997, *AJ* 114, 246

Howk, J. C. & Savage, B. D. 1999, *AJ*, 117, 2077

Howk, J. C. 2005 , in *Extra-Planar Gas*, ed. R. Braun, (San Francisco: ASP), p. 287

Norman, C. A. & Ikeuchi, S. 1989, *AJ* 345, 372-383

Perley, R.A, Schwab, F. R. & Bridle, A.: 1989, *Synthesis Imaging in Radio Astronomy*

Scoville, N. Z., et al. 1992, *AJ* 404, L59-L52

Scoville & Young, 1991, *Annual Review of Astro. And Astro.*, **29**, 581-625